Phase Separation Behavior and Morphologies of PMMA/Poly(styrene-*co*-acrylonitrile)/Clay Nanocomposites Prepared by Solution Mixing

Minho Lee, Kyunghoon Lee, Byong Hun Min, Jeong Ho Kim

Department of Chemical Engineering, University of Suwon, Gyeonggi-do, Korea

Received 2 September 2008; accepted 4 August 2009
DOI 10.1002/app.31241
Published online 2 March 2010 in Wiley InterScience (www.interscience.wiley.com).

ABSTRACT: Nanocomposites of blends of PMMA and poly(styrene-*co*-acrylonitrile) (SAN) with natural (PM) or organically modified montmorillonite clays (Cloisite 30B, 25A, and 15A) were prepared by solution mixing and the effect of clay on the phase separation behavior along with morphologies of nanocomposites was investigated. Nanocomposites containing clay C30B prepared from methyl ethyl ketone showed the noticeable decrease in the cloud points. None of the other nanocomposites showed the increase in the cloud point. Location of clay particles in the phase separated matrix is observed to be different depending on the type of clays and solvents. The lowest cloud point of nanocomposites containing C30B may arise from the good dispersion of C30B where Clay C30B may act as the nucleating agent inducing phase separation. Dynamic mechanical and thermal analyses support above observations. © 2010 Wiley Periodicals, Inc. J Appl Polym Sci 117: 49–57, 2010

Key words: nanocomposites; phase behavior; morphology

INTRODUCTION

Polymeric nanocomposites containing organically modified clays have been extensively studied due to various excellent properties that can be achieved compared with conventional composites.[1–5] Although polymer/clay nanocomposites have been widely studied using different preparation methods, such as, *in situ* polymerization, solution blending, and melt mixing,[6–10] a number of studies on the nanocomposites of polymer blends with clays have been recently reported in the literature.[11–30] Various properties of nanocomposites are largely related to the interaction behavior of clays at the interface with polymers. In this regard, it becomes more complicated and even more interesting when it comes to the nanocomposites of polymer blends with clays because there are more interfaces involved in this case than nanocomposites of a single polymer with clays. Even in the case of the solution blending, various dispersion state of clay in nanocomposites can be obtained depending on the type of solvent used.

In the previous studies on nanocomposites of polymer blends with clays, mainly the morphologies of immiscible blend component polymers in the nanocomposites were investigated and the clays were reported to act as compabilizers for the immiscible blends in some cases[20,24,25] but few studies are found on the effect of clay on the phase separation behavior, such as, on the cloud points of the miscible blends. In this study, the effect of clays on the cloud points and morphologies of nanocomposites of blends of PMMA and SAN containing clays were investigated. PMMA and SAN were known to form a miscible blend.

In PMMA nanocomposites, clays are reported to be intercalated or exfoliated depending on the preparation methods.[31–33] Studies on nanocomposites of poly(styrene-*co*-acrylonitrile) (SAN) with clays are also reported in the literature where clays are observed to be intercalated in SAN matrices.[34–36] It is well-known that the mixture of PMMA and SAN forms a miscible blend and the origin of miscibility of PMMA/SAN blends has been suggested to be the repulsion effect between styrene and acrylonitrile units in SAN. It means that the miscibility of the blend is not very strong compared with the ones with specific interactions between the blend components.[37,38] PMMA is reported to be miscible with SAN depending on the AN composition in the range from 9.4 up to 34.4 wt % of AN in SAN.[39–45] PMMA/SAN blends were reported to show the lower critical solution temperature (LCST) behavior. The cloud point for 50/50 blend is known to be around 180°C.[46]

In our previous study,[47] nanocomposites of PMMA/SAN blends with nanoclays were prepared by melt mixing in the twin screw extruder where

Correspondence to: J. H. Kim (jhkim@suwon.ac.kr).

TABLE I
Sample Designation of PMMA/SAN/Clay Nanocomposites

Polymer and clay composition (wt %)						Sample designation	
PMMA	SAN	PM[a]	C30B	C25A	C15A	Samples prepared from MEK	Samples prepared from chloroform
50	50	–	–	–	–	P/S (M)	P/S (C)
47.5	47.5	5	–	–	–	P/S-PM (M)	P/S-PM (C)
47.5	47.5	–	5	–	–	P/S-30B (M)	P/S-30B (C)
47.5	47.5	–	–	5	–	P/S-25A (M)	P/S-25A (C)
47.5	47.5	–	–	–	5	P/S-15A (M)	P/S-15A (C)

[a] PM, pristine montmorillonite.

the melt mixing temperature of nanocomposites were above the LCST of the blend and the morphology of the resulting phase separated blends were reported.

In this study, nanocomposites of PMMA/SAN blends with clays were prepared by solution blending, where the difference with our previous study is that the nanocomposites can be prepared without phase separation as they are mixed with clays at room temperature below the cloud point of the blend. Effect of clays modified with different organic modifiers on the phase separation temperature and the morphology of nanocomposites as well as the effect of different solvent on clay dispersion in the nanocomposites are investigated in this study. Clays used were pristine montmorillonite Cloisite® Na^+ (PM) in natural form and modified clays Cloisite® 30B (C30B), Cloisite® 25A(C25A), and Cloisite® 15A(C15A) with cationic–organic surfactants.

Two different solvents used in solution mixing were methyl ethyl ketone (MEK) and chloroform. MEK is reported to give a homogeneous miscible blend of PMMA and SAN, but chloroform is not. Phase separated blends are known to be obtained due to so-called solvent effect when chloroform is used in the solution of PMMA and SAN even at the room temperature, but chloroform is also used in this study because C25A and C15A are well dispersed in chloroform but not in MEK.

Various analyses were carried out using X-ray diffraction (XRD), transmission electron microscopy (TEM), differential scanning calorimetry (DSC), and dynamic mechanical analysis (DMA).

EXPERIMENTAL

Materials

The polymers used in this study were PMMA (LG Chem., melt index: 5.8) and SAN25 (AN content: 26 wt %, LG Chem., melt index: 10). Solvents used were methyl ethyl ketone (MEK, Samchun Pure Chemical Co.) and chloroform (Samchun Pure Chemical Co.). Clays used in this study were pristine montmorillonite Cloisite® Na^+ in natural form (PM) and modified clays Cloisite® 30B (C30B), Cloisite® 25A(C25A), and Cloisite® 15A(C15A) with cationic–organic surfactants. Clays, PM (Cation exchange capacity (CEC): 92.6 meq/100 g), C30B (CEC: 90 meq/100 g), C25A (CEC: 95 meq/100 g), and C15A (CEC: 125 meq/100 g) were obtained from Southern Clay Products. C30B, C25A, and C15A were clays modified with methyl, tallow, bis-2-hydroxyethyl, quaternary ammonium; dimethyl, hydrogenated tallow, 2-ethylhexyl quaternary ammonium ion; and dimethyl, dehydrogenated tallow quaternary ammonium ion, respectively. Clay C15A has the highest hydrophobicity.

Preparation of PMMA/SAN/clay nanocomposites

PMMA and SAN were dried for 4 h at 80°C in the drying oven and all clays were also dried before use for 24 h in the vacuum oven to remove any moisture. The clay loading of all nanocomposite samples was set at 5 wt %. Solvents MEK and chloroform were used without any further purification. A solution of 5 wt % clay in MEK or chloroform was sonicated before being added to the solution of PMMA/SAN (50/50 by weight) in MEK or chloroform followed by stirring for 24 h at room temperature. The mixture was then cast onto aluminum foil and the resulting films were dried at room temperature for 48 h followed by subsequent drying for 72 h under vacuum. Samples, thus, prepared were listed in Table I. Hereinafter, nanocomposites of PMMA/SAN with clays prepared from MEK or chloroform solution will be described as P/S-clay abbreviation (M) or P/S-clay abbreviation (C), respectively, such as, PMMA/SAN with C15A prepared using MEK will be described as P/S-15A (M).

Characterization and measurements

The change in gallery distance of silicate layers in the clay was determined on X-ray diffractometer (D-8 Advance) using CuKα radiation at 40 kV, 35 mA. The samples were scanned at 2°/min. The basal

TABLE II
Cloud Points of PMMA/SAN/Clay Nanocomposites

Nanocomposites from MEK	Cloud point (°C)	Nanocomposites from chloroform	Cloud point (°C)
P/S (M)	186 ± 1.0	P/S (C)	–
P/S-PM (M)	187 ± 0.5	P/S-PM (C)	–
P/S-30B (M)	181 ± 2.0	P/S-30B (C)	–
P/S-25A (M)	182 ± 1.5	P/S-25A (C)	–
P/S-15A (M)	185 ± 1.0	P/S-15A (C)	–

spacing of the clay, d_{001} was calculated using the Bragg's law ($\lambda = 2d\sin\theta$).

TEM images of nanocomposite specimens were obtained using energy filtering TEM (LEO-912AB OMEGA, LEO) with accelerating voltage of 120 kV at the Korea Basic Science Institute. TEM specimens were prepared by encapsulating nanocomposites in the epoxy resin and ultramicrotoming using a diamond knife at room temperature.

The cloud points of nanocomposite samples were measured by visual inspection on a hot plate by heating the samples from room temperature to 300°C at a heating rate of 2°C/min.

The glass transition temperatures were measured by differential scanning calorimetry (DSC, TA Instrument DSC2010). DSC samples of 10 mg masses were heated in nitrogen atmosphere at a heating rate of 20°C/min. DMA was performed at a tension mode using Seiko Exstar 6000 DMA/SS6100 (SEICO Instrument, Japan). The temperature sweep mode was performed in the interval between 30 and 180°C at the heating rate of 5°C/min with 1 Hz frequency.

RESULTS AND DISCUSSION

Cloud points of PMMA/SAN/clay nanocomposites

To see the effect of clays on the phase behavior of nanocomposites of polymer blends with clays, cloud points were measured by heating nanocomposite samples prepared at room temperature.

Blend samples of PMMA and SAN without any clays prepared using MEK were transparent indicating a homogeneous miscible blend. The cloud point of this PMMA/SAN [P/S (M): (M) indicates MEK] was measured to be 186°C as shown in Table II. The cloud points of P/S-PM (M) and P/S-C15A(M) were observed to be 187°C and 185°C, which are almost same as that of PMMA/SAN without any clays [P/S (M)]. This exhibits that clays PM or C15A do not give much effect on the phase behavior of PMMA/SAN blends.

Cloud points of nanocomposites containing C30B and C25A prepared from MEK were observed to be 181°C and 182°C, respectively, which are lower than that of PMMA/SAN without any clays. This indicates that clays C30B or C25A affect the phase separation behavior of blends of PMMA/ SAN.

Because chloroform gave phase separated opaque films at room temperature as previously reported in the literature, cloud points could not be measured for the samples prepared from chloroform including samples without any clays or the ones containing PM, C30B, C25A, and C15A.

In the previous studies on some nanocomposites of immiscible polymer blends, clays are reported to decrease the phase separated domain sizes.[9,20,24,25] It is noted that though the domain sizes of immiscible blends decrease in those studies, clays do not make the blends completely miscible and accordingly cloud points cannot be measured. Also, whether the reason for the decrease in domain sizes is due to the clays acting as compatibilizers in the real thermodynamic sense or due to the change in viscosity ratio of two separated phases by the addition of clays is still not quite clear.

This study deals with the clays not in the immiscible blends but in the miscible blends of PMMA/SAN. To analyze the results of cloud point measurements in view of the morphology of the nanocomposites, TEM pictures were taken.

Morphology of PMMA/SAN/clay nanocomposites

The morphology of nanocomposites were examined by using TEM in order to observe the dispersion state of silicate layers and the separated polymer phases, if any. Figure 1(a–d) show TEM images of nanocomposites prepared from MEK containing 5 wt % clays PM, C30B, C25A, and C15A, respectively. Poor dispersion of clay PM was observed as shown in Figure 1(a). In the meantime, clay C30B is observed to be very well dispersed in PMMA/SAN matrix close to exfoliation as shown in Figure 1(b). TEM pictures for P/S/25A in Figure 1(c) also showed a good dispersion of clays in the matrix of PMMA and SAN.

These two nanocomposites with C30B or C25A exhibiting good clay dispersion showed the lower cloud point than PMMA/SAN without any clay. This indicates that clays can induce phase separation in miscible blends, whereas clays can reduce the separated domain size in some of the previous studies on immiscible blends.

Because clay C30B or C25A is well dispersed in the matrix as shown in Figure 1(b) or Figure 1(c), C30B or C25A may be thought to have some interaction with PMMA or SAN accelerating phase separation. In these nanocomposites, clay C30B or C25A may be thought to act as a nucleating agent for phase separation. Clays are reported in the previous studies to act as nucleating sites in some nanocomposites containing polymer blends.[11,16,18]

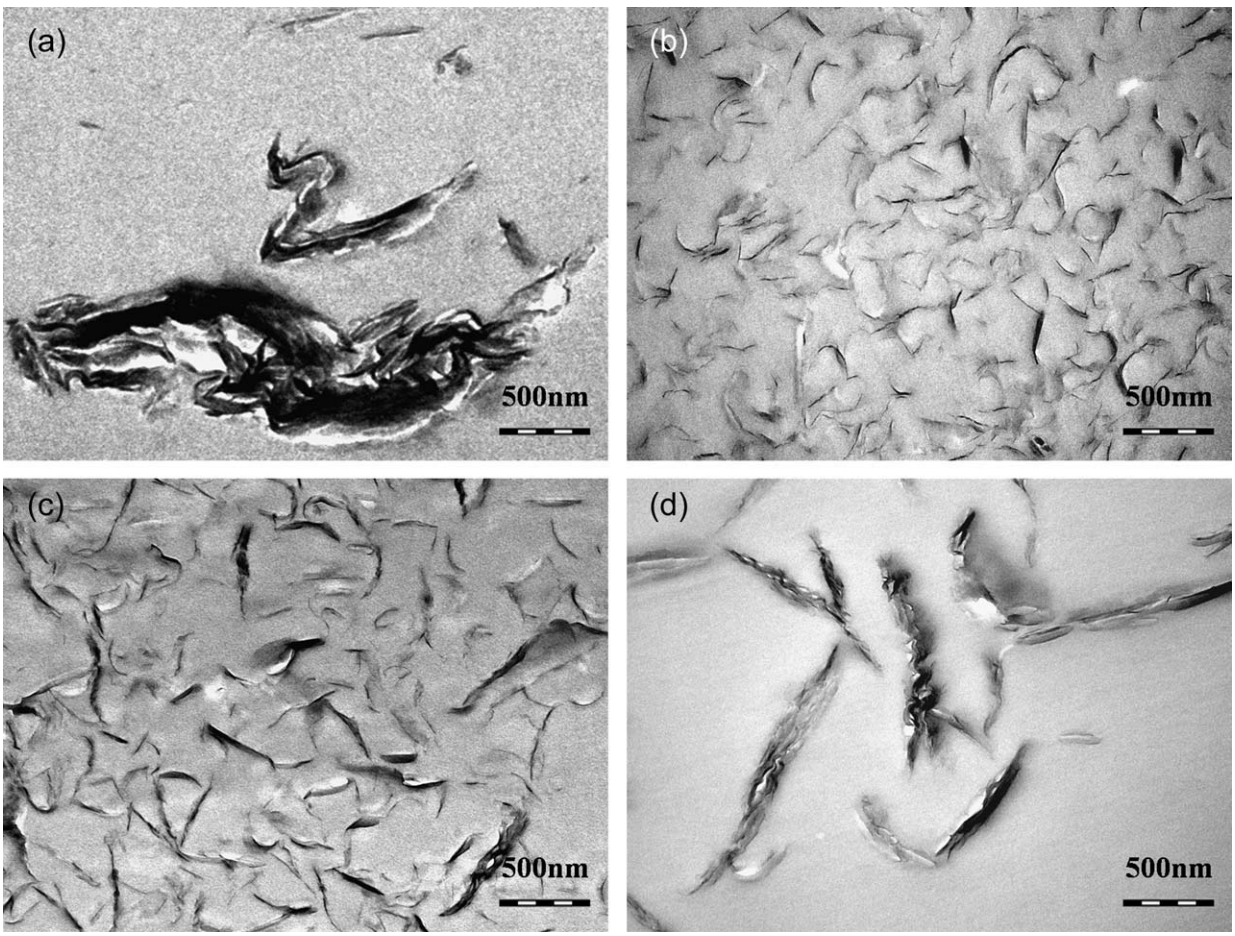

Figure 1 TEM images of nanocomposites prepared from MEK containing 5 wt % of (a) PM, (b) C30B, (c) C25A, and (d) C15A.

Clays PM and C15A in Figures 1(a,d) show a poor dispersion in PMMA/SAN matrix as expected because PM and C15A were not well dispersed in MEK during nanocomposite preparation as well as their poor compatibility with PMMA or SAN. This means that clays PM and C15A do not affect the phase behavior of PMMA/SAN blend, which is consistent with the result of little change in cloud points of nanocomposites containing PM or C15A. To see the different dispersion state of clay dispersion in the different solvent, various clays were mixed with MEK or chloroform by magnetic stirring. Among various clays used in this study, only C30B was well dispersed in MEK and clay C25A showed a fair dispersion in MEK as shown in Figure 2(a). In chloroform, only clay C15A showed a good dispersion as shown in Figure 2(b).

Good dispersion of clay C30B in PMMA/SAN nanocomposites was expected since increase in interlayer spacing of C30B in PMMA or in SAN was reported in the previous studies on nanocomposites of PMMA or SAN with various clays[33–45] as well as the fact that C30B is well dispersed in MEK during nanocomposite preparation. Similar to C30B but less degree of increase in interlayer spacing of C25A in PMMA or in SAN than C30B was also reported in the literature.[33,34,36,48–57]

Cloud points of P/S-PM (M) (187°C) and P/S-C15A (M) (185°C) were about the same as that (186°C) of PMMA/SAN without any clay indicating that PM or C15A does not give much effect on phase separation due to its poor dispersion in the matrix. This is consistent with the poor dispersion of clays PM or C15A in TEM pictures.

Figure 3(a–d) show TEM images of nanocomposites prepared from chloroform containing 5 wt % clays PM, C30B, C25A, and C15A, respectively. Morphologies of nanocomposites containing C30B [Fig. 3(b)] and of the ones containing C25A [Fig. 3(c)] are very similar to those of corresponding nanocomposites prepared from MEK shown in Figure 1(b,c), respectively, except that Figure 3(b,c) show the phase separated structures due to the use of chloroform as a solvent.

Because C30B is not well dispersed in chloroform during the nanocomposite preparation as shown in Figure 2(b), the good dispersion of C30B in Figure 3(b) reveals that the dispersibility of clay in the

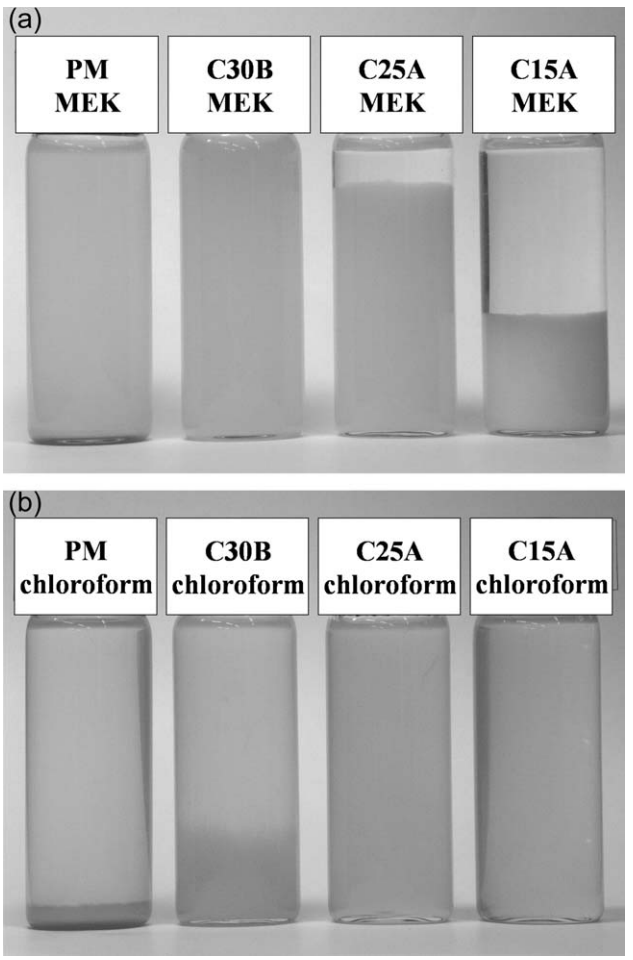

Figure 2 Suspension state of PM, C30B, C25A, and C15A in (a) MEK and (b) chloroform.

solvent during nanocomposite preparation is not a prerequisite for good dispersion of clay in the final nanocomposite. It rather indicates that the compatibility between matrix polymers and clays plays a more important role in the dispersion of clay in the final nanocomposites.

Phase separation induced by chloroform in P/S-30B(C) was not clearly seen at the high magnification picture in Figure 3(b) but microphase separated structures are observed at a lower magnification picture shown in the inset of Figure 3(b).

Dispersion of PM in Figure 3(a) is again not as good as that in Figure 1(a) and the macrophase separation in this nanocomposite is not seen at this magnification.

For PMMA/SAN nanocomposites containing C15A, very good dispersion close to exfoliation was observed as shown in Figure 3(d), which is quite different from the one prepared from MEK shown in Figure 1(d). Also, clear phase separation cannot be observed in this TEM picture although the cloud point cannot be measured due to the translucent nature of the P/S-C15A(C) samples. This indicates that the phase separation due to chloroform solvent is somewhat retarded in this C15A nanocomposites due to the dispersion of C15A. It is not quite clear at this stage whether the good dispersion of C15A in P/S-15A(C) originates only from the good dispersion of C15A in chloroform solvent followed by the difficulty in restacking of C15A clay layers during nanocomposite preparation due to the high viscosity of nanocomposites or also from the good compatibility between PMMA/SAN and C15A. But considering that C15A nanocomposites prepared from MEK did not show a good dispersion of C15A, whereas C30B nanocomposites prepared from chloroform showed a good dispersion of C30B regardless of solvents, clays C15A are thought not to have a strong affinity with either PMMA or SAN. It follows that good dispersion of C15A may be mainly due to the good dispersion of clay C15A in chloroform during nanocomposites preparation and more possibilities are put on the viscosity issue than the compatibility one.

Although the weak interaction was reported to exist from FTIR analysis between carbonyl groups in PMMA and clays modified with tetra-alkyl di-tallow ammonium salt which is similar to the organic modifier of C15A in the literature,[46] almost no changes in the interlayer distance of clay C15A are reported in PMMA/C15A or SAN/C15A nanocomposites.[33,34] It indicates that the interaction between PMMA/SAN and C15A may be rather very weak, if any. As C15A has a fairly large amount of excess hydrophobic modifiers covering the almost entire clay surface as can be seen by the poor dispersion in MEK in Figure 2(b), chances of interaction between C15A and polar PMMA/SAN may be low. In the cases of PMMA/SAN with C30B or C25A where the compatibility between PMMA/SAN and clays may be better than C15A nanocomposites, cloud points became lower than that of PMMA/SAN without any clay, where clays C30B or C25A are thought to act as a nucleating agent for phase separation. Even if clay C15A acts as a nucleating agent, its effect may be much less than C30B or C25A that has higher affinity with PMMA or SAN although it cannot be proved in P/S-15A(C), which has the phase separated structure from the beginning due to the chloroform solvent. During nanocomposites preparation, good dispersion of C15A in PMMA/SAN may rather retard the phase separation due to the increase in matrix viscosity although this cannot completely prevent the phase separation in true thermodynamic sense.

The phase separated structure in the P/S-30B(C) sample as prepared was observed even by optical microscope as shown in Figure 4. This again indicates that more phase separation was induced by C30B compared with other clays explaining the lowest cloud point of P/S-30B(C).

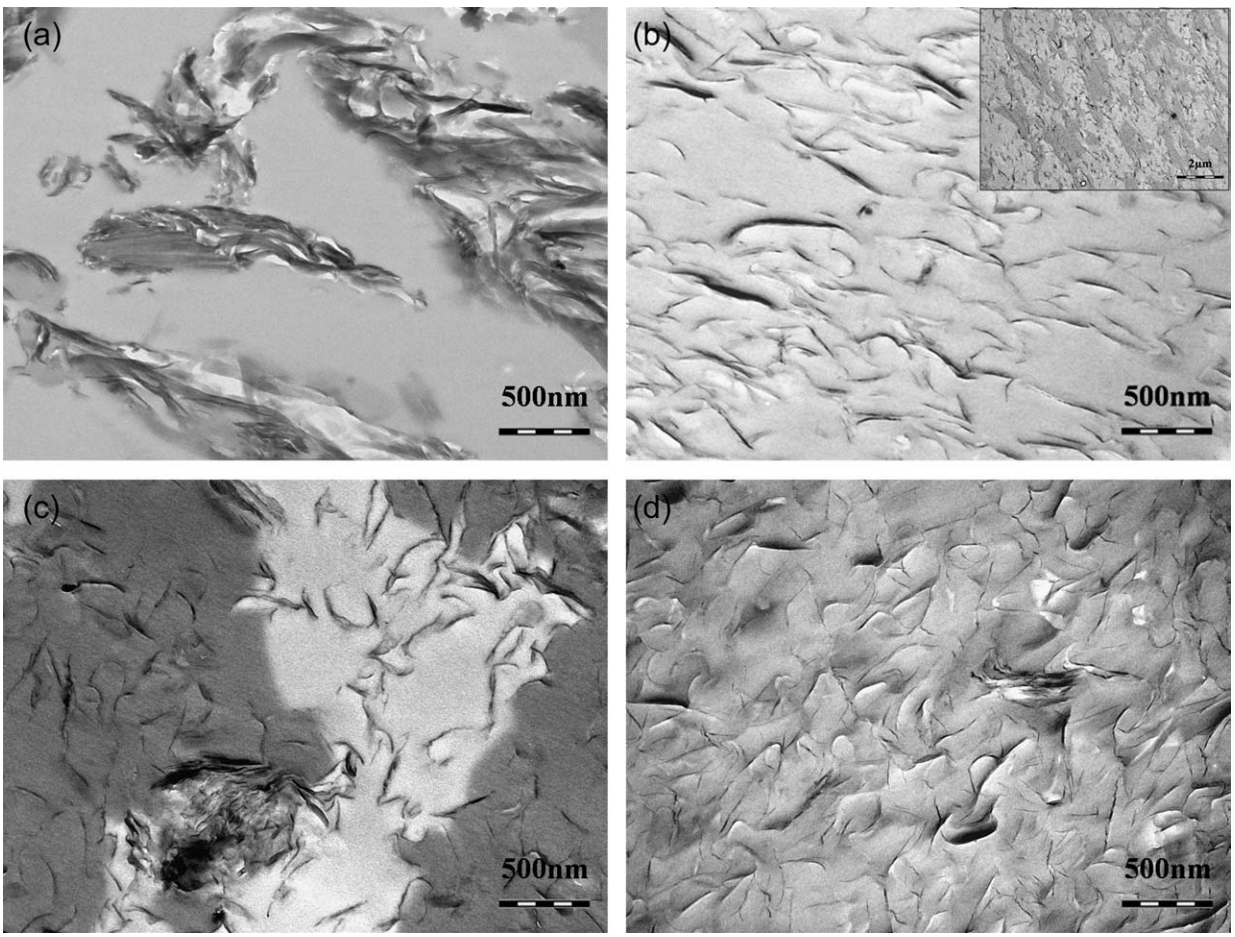

Figure 3 TEM images of nanocomposites prepared from chloroform containing 5 wt % of (a) PM, (b) C30B, (c) C25A, and (d) C15A.

XRD results of PMMA/SAN/clay nanocomposites

Figure 5(a,b) exhibit the XRD results of P/S-30B and P/S-15A, respectively, prepared from both MEK and chloroform. As expected from the TEM observations, no noticeable peaks were observed for both P/S-30B(M) or P/S-30B(C). Although some peaks were observed in P/S-15A(M), XRD results for P/S-15A(C) does not exhibit any peaks also as expected from the good dispersion of C15A in PMMA/SAN prepared from chloroform in TEM pictures. These XRD results support the TEM results in terms of clay dispersion.

Dynamic mechanical properties of PMMA/SAN/clay nanocomposites

Dynamic mechanical properties of the PMMA/SAN nanocomposites were measured to investigate the effect of the clay on the dynamic mechanical behavior. The storage modulus and tan δ results for the PMMA/SAN nanocomposites prepared from MEK are shown in Figure 6(a,b), respectively. Nanocomposites P/S-30B(M) containing C30B exhibit the highest dynamic mechanical storage modulus (E') in the temperature range studied as shown in Figure 6(a). This is consistent with the TEM results where

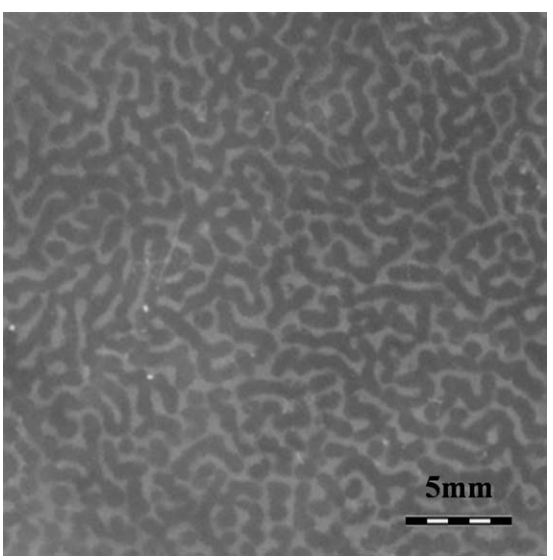

Figure 4 Phase separated structure of P/S-30B(C) observed by optical microscope.

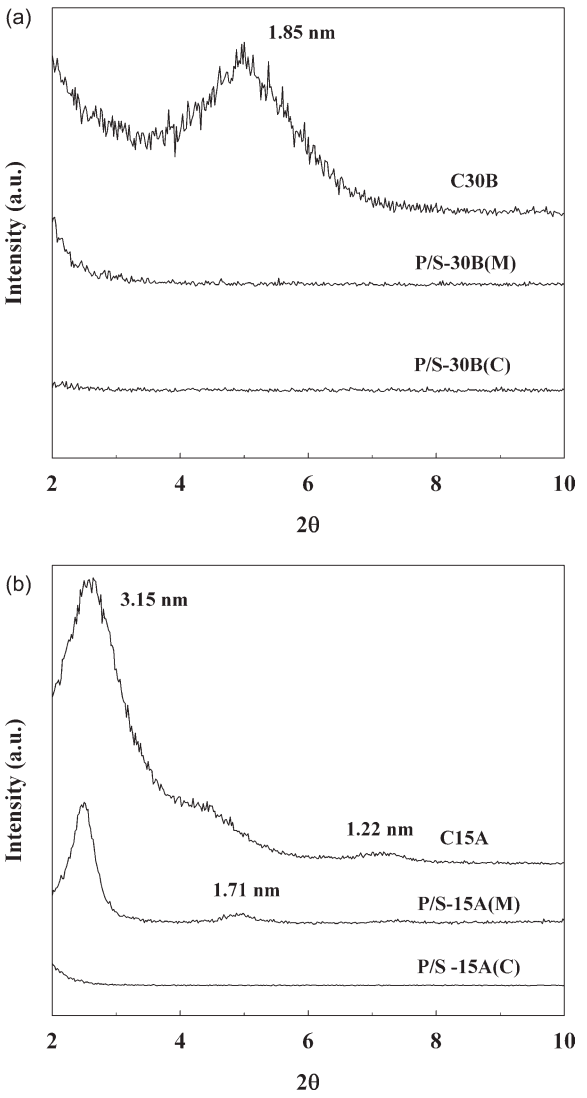

Figure 5 X-ray diffraction patterns of PMMA/SAN/clay nanocomposites containing 5 wt % of (a) C30B and (b) C15A.

C30B nanocomposites show the best dispersion of clays throughout the entire matrix. Lowest modulus of P/S-15A(M) was thought to be due to the low molecular weight modifiers released from C15A which has excess modifiers. Breadth of tan δ in Figure 6(b) may be considered to indicate the homogeneity of the matrix phase. The wider tan δ may be the manifestation of less homogeneity in the matrix. PMMA/SAN without any clay exhibit the narrowest breadth of transition indicating the homogeneous miscible blend. PMMA/SAN nanocomposites containing clays show broader tan δ than PMMA/SAN without clays indicating that clays induce the phase separation.

The storage modulus and tan δ results for the PMMA/SAN nanocomposites prepared from chloroform were shown in Figures 7(a,b), respectively. Storage modulus of PMMA/SAN without any clays show the minimum value exhibiting phase separation between PMMA and SAN when prepared from chloroform. Storage modulus of P/S-15A(C) does not show the lowest value among all nanocomposites containing various clays in this case. This is consistent with the TEM observation where C15A clays were well dispersed in P/S-15A(C). This is again manifested in Figure 7(b) in which the breadth of tan δ for P/S-15A(C) shows the minimum indicating some degree of retardation in phase separation by well dispersed clays C15A in this nanocomposite.

Thermal properties of PMMA/SAN/clay nanocomposites

The criterion for miscibility frequently used is the appearance of a single glass transition temperature, T_g in the blend.[17] Figures 8(a,b) exhibit the DSC results obtained from the first run for the PMMA/

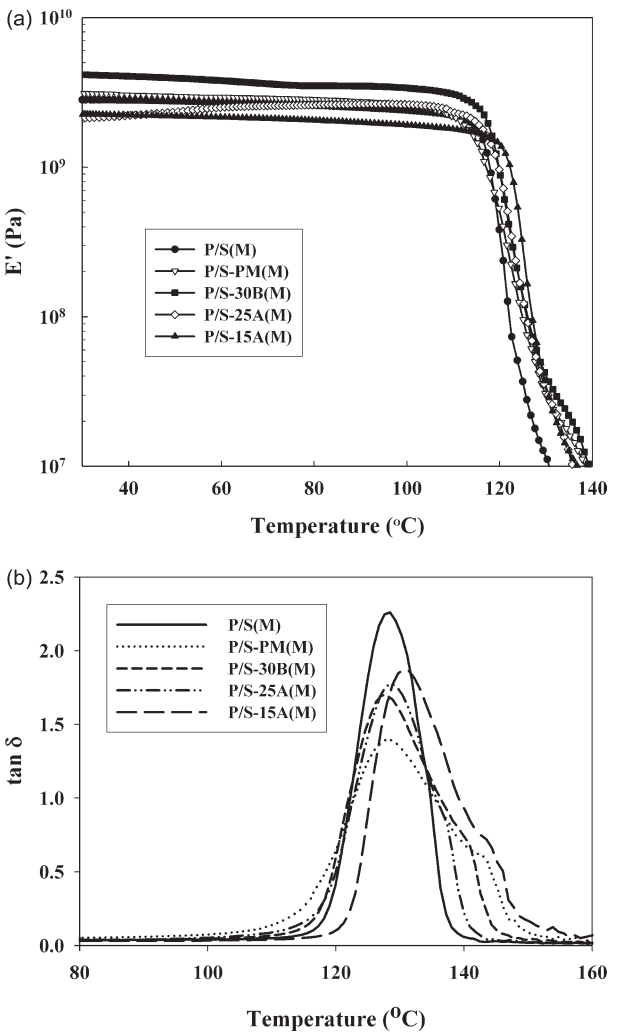

Figure 6 (a) Storage modulus and (b) tan δ versus temperature obtained from dynamic mechanical analysis measurements for PMMA/SAN/clay nanocomposites prepared using MEK.

SAN/clay nanocomposites prepared from MEK and chloroform, respectively. Because the glass transition temperatures of PMMA and SAN used in this study show similar values around 105°C, PMMA obtained from Sigma-Aldrich Corporation having T_g around 120°C was used to prepare the nanocomposite samples for DSC analysis.

Nanocomposites prepared from MEK show the only one glass transition temperature as shown in Figure 8(a) which is the characteristic feature of miscible blends. As can be seen from Figure 8(b), PMMA/SAN without any clay prepared from chloroform shows two distinct glass transition temperatures indicating phase separated structures. PMMA/SAN containing PM or C30B also exhibits two distinct glass transition temperatures which is consistent with TEM results. Broad transition region was observed for P/S-25A(C) indicating two microphase separated structure. Almost single T_g was observed for P/S-15A(C) indicating that clay C15A appears to retard phase separation consistent with the DMA results as well as the TEM picture.

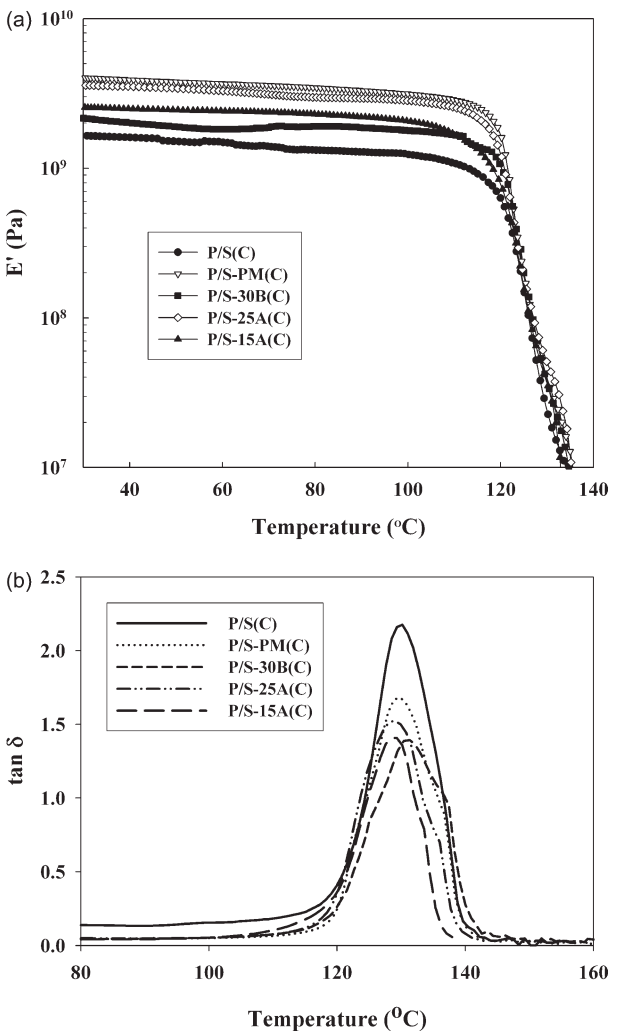

Figure 7 (a) Storage modulus and (b) tan δ versus temperature obtained from dynamic mechanical analysis measurements for PMMA/SAN/clay nanocomposites prepared using chloroform.

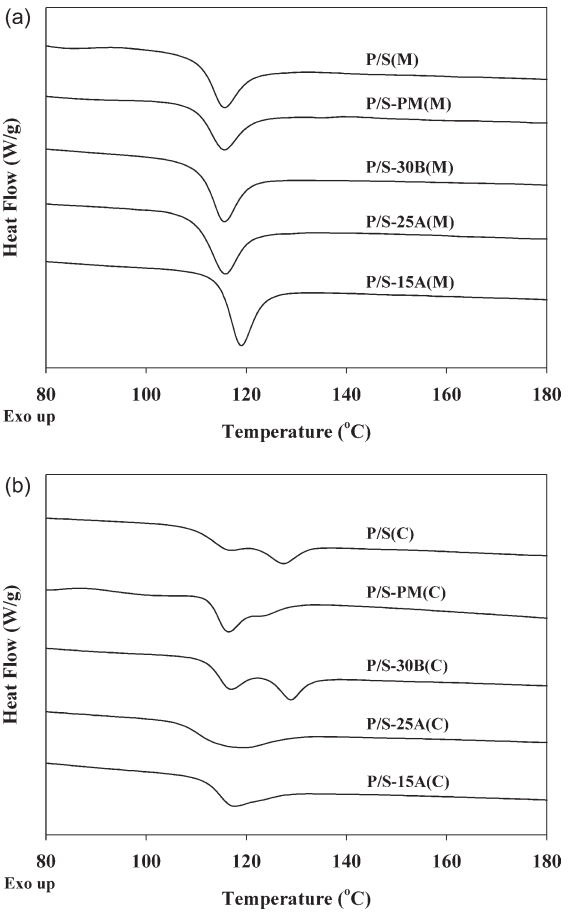

Figure 8 DSC thermograms of PMMA/SAN/clay nanocomposites prepared from using (a) MEK and (b) chloroform.

CONCLUSIONS

PMMA and SAN form a miscible blend prepared using MEK as a solvent and the cloud points can be measured. All nanocomposites prepared using MEK showed the decrease in the cloud points except the one containing natural clay PM. Especially, noticeable decrease in the cloud point was observed in nanocomposites containing C30B and similar but less degree of decrease was shown in the C25A case. In both nanocomposites, good dispersion of clays in the polymer matrix was observed in TEM results. This indicates that well dispersed clays can facilitate the phase separation resulting in lower cloud points. Clays may be thought to act as a nucleating agent inducing phase separation.

Nanocomposites prepared using chloroform as a solvent exhibited the phase separated morphologies due to the solvent effect and the cloud points cannot be measured although clays C30B and C15A

exhibited a fairly good dispersion in TEM pictures. From these observations, clay C30B turns out to have the best compatibility with PMMA/SAN among various clays tested because C30B exhibits a good dispersion in PMMA/SAN nanocomposites though C30B is not well dispersed in chloroform during nanocomposites preparation.

Storage modulus and tan δ results in DMA and the breadth of transition in thermal analysis are consistent with above findings.

References

1. Messersmith, P. B.; Giannelis, E. P. Chem Mater 1994, 6, 1719.
2. Kojima, Y.; Usuki, A.; Kawasumi, M.; Okada, A.; Fujushima, A.; Kurauchi, T.; Kamigaito, O. J Mater Res 1993, 8, 1185.
3. Mirabella, F. M., Jr. Dekker Encyclopedia of Nanoscience and Nanotechnology; Marcel Dekker, Inc.: New York, 2004; pp 3015–3030.
4. Noval, B. Adv Mater 1993, 5, 422.
5. Burnside, S. D.; Giannelis, E. P. Chem Mater 1995, 7, 1597.
6. Vaia, R. A.; Giannelis, E. P. Macromolecules 1997, 30, 8000.
7. Park, J.; Jana, S. C. Macromolecules 2003, 36, 2758.
8. Park, J.; Jana, S. C. Polymer 2004, 45, 7673.
9. Mehta, S.; Mirabella, F. M.; Rufener, K.; Bafna, A. J Appl Polym Sci 2004, 92, 928.
10. Huang, X.; Lewis, S.; Brittain, W. J.; Vaia, R. A. Macromolecules 2000, 33, 2000.
11. Chow, W. S.; Ishak, M.; Karger-Kocsis, J. J. J Polym Sci Part B Polym Phys 2005, 43, 1198.
12. Zou, H.; Zhang, Q.; Tan, H.; Ke, W.; Du, R.; Fu, Q. Polymer 2006, 47, 6.
13. Khatua, B. B.; Lee, D. J.; Kim, H. Y.; Kim, J. K. Macromolecules 2004, 37, 2454.
14. Hong, J. S.; Namkung, H.; Ahn, K. H.; Lee, S. J.; Kim, C. Y. Polymer 2006, 46, 3967.
15. Dharaiya, D. P.; Jana, S. C. J Polym Sci Part B Polym Phys 2005, 43, 3638.
16. González, I.; Eguiazábal, J. I.; Nazábal, J. Eur Polym J 2006, 42, 2905.
17. Ray, S. S.; Bandyopadhyay, J.; Bousmina, M. Macromol Mater Eng 2007, 292, 729.
18. Yoo, Y. J.; Park, C. H.; Lee, S. G.; Choi, K. Y.; Kim, D. S.; Lee, J. H. Macromol Chem Phys 2005, 206, 878.
19. Fang, Z.; Xu, Y.; Tong, L. Polym Eng Sci 2007, 47, 551.
20. Ray, S. S.; Bousmina, M. Macromol Rapid Commun 2005, 26, 450.
21. Kontopoulou, M.; Liu, Y.; Austin, J. R.; Scott Parent, J. Polymer 2007, 48, 4520.
22. Ray, S. S.; Pouliot, S.; Bousmina, M.; Utrachi, L. A. Polymer 2004, 45, 8403.
23. Ray, S. S.; Bousmina, M. Macromol Rapid Commun 2005, 26, 1639.
24. Si, M.; Araki, T.; Ade, H.; Kilcoyne, A. L. D.; Fisher, R.; Sokolov, J. C.; Rafailovich, M. H. Macromolecules 2006, 39, 4793.
25. Su, Q.; Feng, M.; Zhang, S.; Jiang, J.; Yang, M. Polym Int 2007, 56, 50.
26. Li, Y.; Shimizu, H. Macromol Rapid Commun 2005, 26, 710.
27. Li, Y.; Shimizu, H. Polymer 2004, 45, 7381.
28. Lipatov, Y. S.; Nesterov, A. E.; Ignatova, T. D.; Nesterov, D. A. Polymer 2002, 43, 875.
29. Wang, Y.; Zhang, Q.; Fu, Q. Macromol Rapid Commun 2003, 24, 231.
30. Calcagno, C. I. W.; Mariani, C. M.; Teixeira, S. R.; Mauler, R. S. Compos Sci Technol.
31. Lee, D. C.; Jang, L. W. J Appl Polym Sci 1996, 61, 1117.
32. Chen, G.; Chen, X.; Lin, Z.; Yao, K. J. J Mater Sci Lett 1999, 18, 1761.
33. Okamoto, M.; Moritta, S.; Taguchi, H.; Kim, Y. H.; Kotaka, T.; Tateyama, H. Polymer 2000, 41, 3887.
34. Kim, J. W.; Jang, L. W.; Choi, H. J.; Jhon, M. S. J Appl Polym Sci 2003, 89, 821.
35. Lee, S.-S.; Lee, C. S.; Kim, M.-H.; Kwak, S. Y.; Park, M.; Lim, S.; Choe, C. R.; Kim, J. J Appl Polym Sci 2001, 39, 2430.
36. Chu, L.-L.; Anderson, S. K.; Harris, J. D.; Beach, M. W.; Morgan, A. B. Polymer 2004, 45, 4051.
37. Kambour, R. P.; Bendler, J. T.; Bopp, R. C. Macromolecules 1983, 16, 753.
38. Paul, D. R.; Barlow, J. W. Polymer 1984, 25, 487.
39. Suess, M.; Kressler, J.; Kammer, H. W. Polymer 1987, 28, 957.
40. Nishimoto, N.; Keskkula, H.; Paul, D. R. Polymer 1989, 30, 1279.
41. Cowie, J. M. G.; Reid, V. M. C.; Mcewen, I. J. Polymer 1990, 31, 486.
42. Fowler, M. E.; Keskkula, H.; Paul, D. R. Polymer 1987, 28, 1703.
43. Fowler, M. E.; Barlow, J. W.; Paul, D. R. Polymer 1987, 28, 2145.
44. Mcmaster, L. P. Adv Chem Ser 1975, 142, 43.
45. Naito, K.; Johnson, G. E.; Allara, D. L.; Kwei, T. K. Macromolecules 1977, 10, 681.
46. Du, M.; Gong, J.; Zheng, Q. Polymer 2004, 45, 6725.
47. Lee, M. H.; Dan, C. H.; Kim, J. H.; Cha, J.; Kim, S.; Hwang, Y.; Lee, C. H. Polymer 2006, 47, 4359.
48. Stretz, H. A.; Paul, D. R.; Li, R.; Keskkula, H.; Cassidy, P. E. Polymer 2005, 46, 2621.
49. Kumar, S.; Jog, J. P.; Natarajan, U. J Appl Polym Sci 2003, 89, 1186.
50. Shen, Z.; Simon, G. P.; Cheng, Y.-B. J Appl Polym Sci 2004, 92, 2101.
51. Bourbigot, S.; Vanderhart, D. L.; Gilman, J. W.; Bellayer, S.; Stretz, H.; Paul, D. R. Polymer 2004, 45, 7627.
52. Tiwari, R. R.; Natarajan, U. J Appl Polym Sci 2007, 105, 2433.
53. Park, J. H.; Jana, S. C. Polymer 2003, 44, 2091.
54. Zeng, C.; Lee, L. J. Macromolecules 2001, 34, 4098.
55. Kim, S. W.; Jo, W. H.; Lee, M. S.; Ko, M. B.; Jho, J. Y. Polymer 2001, 42, 9837.
56. Wang, D.; Zhu, J.; Yao, Q.; Wilkie, C. A. Chem Mater 2002, 14, 3837.
57. Lee, S.-S.; Lee, C. S.; Kim, M.-H.; Kwak, S. Y.; Park, M.; Lim, S.; Choe, C. R.; Kim, J. J Polym Sci Part B Polym Phys 2001, 39, 2430.